ARTICLES

Electron Hydration Dynamics: Simulation Results Compared to Pump and Probe Experiments

E. Keszei*

Department of Physical Chemistry, Eötvös University, P.O. Box 32, H-1518 Budapest 112, Hungary

T. H. Murphrey and P. J. Rossky

Department of Chemistry and Biochemistry, The University of Texas at Austin, Austin, Texas 78712-1167

Received: February 22, 1994; In Final Form: August 30, 1994[⊗]

Previous analysis of the computer simulation of the relaxation of energetic excess electrons in liquid water (Keszei E.; *et al. J. Chem. Phys.* **1993**, 99, 2004) has led to a detailed molecular level and kinetic picture of this process, including the presence of multiple pathways to the equilibrium ground state. In order to explore the validity of this view, simulation results are directly compared to two available data sets obtained experimentally via ultrafast absorption spectroscopy. The analysis is carried out, first, by convolution of the simulated instantaneous spectral response of the electron with an appropriate instrumental response function. The difference between the resulting data and the reported experimental observations is no larger than the difference between the two experimental data sets. It is further shown by separate analysis that the mechanism of relaxation apparent in the simulation is kinetically consistent with the available experimental data. It is pointed out that a number of available, and apparently different, hypotheses for the sequence of species present during electronic relaxation share key features with this mechanism. Taken together, these considerations support the validity of the microscopic processes evident in simulation and emphasize the limitations inherent in the analysis of the experimentally determined spectral dynamics.

I. Introduction

In a recent paper, Murphrey and Rossky have reported the results of a nonadiabatic quantum dynamical simulation of electron hydration in a water bath containing flexible water molecules.[1] This has been the first simulation whose results were fully compatible with available experimental evidence. The simulation also provided a detailed source of data that made it possible to conduct a thorough statistical analysis. As a result, a new hydration mechanism was inferred in a subsequent paper,[2] which goes beyond those used in published treatments of experimental data.[3−12]

The new mechanism explicitly includes an initial thermalization step and a direct pathway from the delocalized to the relaxed ground state without an intermediate, both of them providing an important contribution to the transient absorbance during the hydration process. This mechanism can be written as

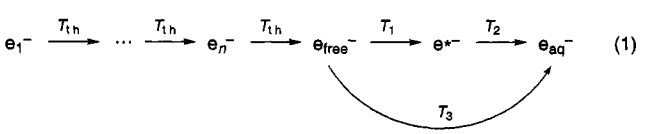

(1)

where e_1^- to e_n^- are the different eigenstates of the manifold of delocalized excited states with less energy as the subscript increases. The species e_{free}^- means a sufficiently low-lying eigenstate of the same manifold which is ready for localization without further energy loss within the manifold of the delocalized states. e_*^- is the (p-like) localized excited state and e_{aq}^- the fully relaxed hydrated electron. Supposing identical characteristic times T_{th} for each thermalization step (as shown in eq 1) and a first-order law for the energy loss during thermalization as well as for subsequent localization steps, the resulting system of kinetic differential equations can be solved to yield concentration functions of the species involved.[2]

The results of the simulation reported in refs 1 and 2 can be fitted very well by using the above mechanism. The estimated parameters T_{th}, T_1, T_2, and T_3 are listed in Table II of ref 2, for electrons injected with about 2.0 and 2.5 eV of excess energy, respectively. The good fit and the statistically significant values of the kinetic parameters obtained completely support the conclusion that mechanism 1 correctly expresses the physical picture underlying the simulation. The purpose of the present study is to compare the inferred kinetic results from the simulation to available ultrafast laser experimental data.

In section II, we briefly describe the experimental results considered in this paper and give an outline of the interpretation of those results published earlier. Section III describes two different methods of comparison of the simulation to the laser experiments. Several consequences of the comparison will be discussed in section IV.

II. Experimental Results

A. Kinetic Traces Measured with the Pump and Probe Laser Technique. The pump and probe laser method does not provide the usual kinetic absorbance curves like simple spectrophotometric methods. The subpicosecond time resolution is based on the variation of the delay between the pump and the

[⊗] Abstract published in *Advance ACS Abstracts,* November 15, 1994.

0022-3654/95/2099-0022$09.00/0

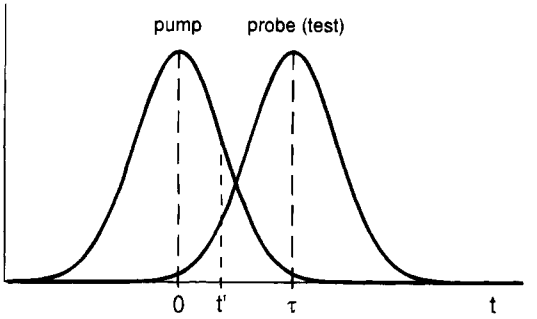

Figure 1. Arrangement of the pump and probe pulses in the ultrafast time-resolved laser experiment, with the notation used in eq 2.

probe pulses, for the response of the measuring electronic device is much longer than the duration of the pulses. As a result, the detected absorbance with a delay τ is

$$A(\tau) = \int_{-\infty}^{\infty} I_t(t' - t) \int_{-\infty}^{t'} I_p^n(t) f(t' - t)\, dt\, dt' \qquad (2)$$

The arrangement of the two pulses can be seen in Figure 1. $I_t(t' - \tau)$ is the intensity of the probe pulse ("test") centered around $t = \tau$, $I_p^n(t)$ is that of the pump pulse centered around $t = 0$ raised to the proper power according to the n-photon excitation,[11] and $f(t' - t)$ is the instantaneous absorbance at time $t' - t$, which can be written as the sum of the absorbances of all the relevant k species:

$$f(t' - t) = \sum_{i=1}^{k} [\epsilon_i c_i(t' - t) l] \qquad (3)$$

according to the Beer–Lambert law. Here, ϵ_i is the molar absorptivity of the ith species, l is the optical path length, and $c_i(t' = t)$ is the concentration of the ith species evolved from the excitation at time t, measured at time t'. Fixing the value of the function $f(t' - t) \equiv 0$ is $t' - t < 0$ (extending thus the upper integration limit from t' to ∞) and changing the order of integration in eq 2, we can find that the detection absorbance is the *convolution* of the instantaneous kinetic function $f(t' - t)$ with the *correlation* of the pump and probe pulses:

$$A(\tau) = \mathrm{corr}(I_p^n, I_t) \otimes f \qquad (4)$$

Now, this convolution results in substantial loss of resolution, as can be seen in Figure 2. The correlation of the two pulses can be considered as the "instrumental resolution" of the pump and probe experimental setup. It is closely related to the original pulse shape of the ultrafast laser source, but this "effective pulse" is at least twice as wide as the source pulse. This convolution makes kinetic inference from pump and probe measurements complicated and makes the comparison with nonconvolved concentration functions an issue of fundamental interest.

B. Results on Electron Hydration Kinetics. Although quite a few ultrafast laser studies of electron hydration have been published in the last decade,[3-11] not all of them are accessible for detailed examination. The published reports of the first experiment of Gauduel *et al.*[4] contain the observed differential optical densities at three suitable wavelengths. At that time, experimental uncertainty was relatively large so that the experimental data can be read from published figures with an uncertainty of less than that inherent in the data. Somewhat later reports of Long *et al.*[9,10] do not provide original observations except at one wavelength (625 nm), so their differential optical density results can only be reconstructed from their published kinetic and optical parameters. Recent publications[5-7]

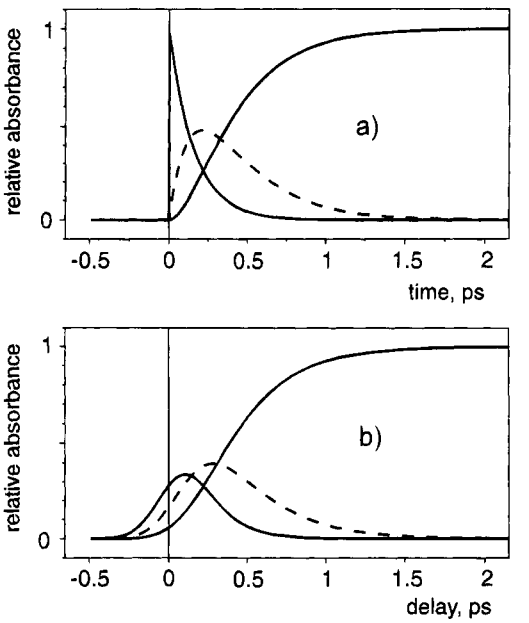

Figure 2. Illustration of the measured kinetic traces for a decomposing reactant, a transient species, and a product species showing the effect of convolution. (a) Instantaneous responses, (b) traces measured with pump and probe method. The earliest evolving species is the reactant, the dashed line shows the transient, and the saturating curve shows the product. Note that the curves do not represent actual experimental data. Showing instantaneous curves and their convolved counterparts, they only illustrate the effect of convolution on simple transient kinetics. However, the parameters of this example are chosen to correspond to the time scales in the experiments considered in this paper.

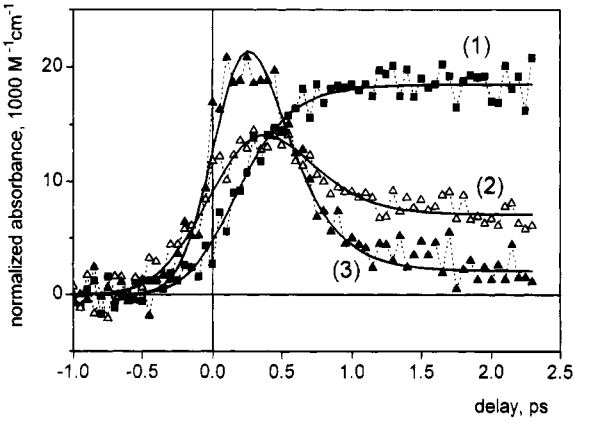

Figure 3. Experimental pump and probe kinetic traces of electron hydration in pure water reported by Gauduel *et al.* at three different wavelengths.[4] Experimental points are interconnected with dotted lines. Solid curve is fitted either with mechanism 1 or mechanism 5. Parameters of the best fit are shown in Table 1. Wavelengths are as follows: (1) 720, (2) 900, and (3) 1250 nm.

usually do not show enough original measured kinetic traces, and even if they do show some, readout errors from the figure might now exceed experimental uncertainties, for experimental precision has been greatly improved recently.

Due to the factors just described, here we shall only deal with two early measurements. Figure 3 shows the kinetic traces measured by Gauduel *et al.*[4] at three wavelengths. At 720 nm, most of the absorption comes from the fully hydrated electron e_{aq}^- (productlike trace). At 1250 nm, the absorbance of the transient species dominates, though there is still some "residual" absorbance of the product present. The intermediate 900-nm curve obviously contains important contributions of both intermediate and product absorbances. These properties indicate that the curves have sufficient information for both the transient

TABLE 1: Comparison of the Kinetic Parameters Obtained with Mechanism 1 from the Simulated Hydration of ~2.5-eV Initial Excess Energy Electrons[2] and from the Experimental Data of Gauduel *et al.*[4a]

parameter	simulation ~2.5 eV, mechanism (1)	Gauduel *et al.* mechanism 1	Gauduel *et al.* two step	Long *et al.* two step
ϵ_{hot}^{720}	2.6	3.6		
ϵ_{free}^{720}	5.2	7.1		
ϵ_{*}^{720}	9.8	13.3	9.6	11.0
ϵ_{hot}^{900}	5.8	14.3		
ϵ_{free}^{900}	10.7	25.7		
ϵ_{*}^{900}	15.1	28.6	36.4	13.9
ϵ_{hot}^{1250}	11.9	29.7		
ϵ_{free}^{1250}	14.0	34.5		
ϵ_{*}^{1250}	14.5	36.6	57.9	10.2
T_{th}	3.1	6		
T_1	92	100	110	180
T_2	67	330	240	540
T_3	48	350		

[a] The latter were calculated using nonlinear least-squares estimation and the method of reconvolution (see section III.A). For comparison, parameters obtained from the same experimental data[12] and those of Long *et al.* with the simple two-step mechanism (eq 5) are also given.

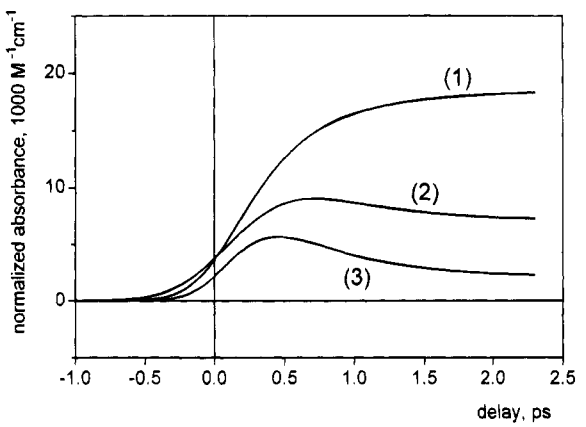

Figure 4. Reconstructed experimental curves obtained with the parameters reported by Long *et al.*[9,10] from their pump and probe electron hydration experiments. The curves are calculated on the basis of the two-step mechanism (eq 5), as published parameters referred to this mechanism. The convolution was carried out with the same effective pulses as in Figure 3. Numbers 1−3 indicate the same wavelengths as in Figure 3. Note that the 1250-nm data were obtained by using some extrapolation of the reported results.

and the product species' kinetic behavior. The authors considered the simplest mechanism which includes transient species, and in fact, it fully describes the kinetic traces within the experimental error. This is the so-called "two step" mechanism:

$$e_{free}^- \xrightarrow{T_1} e_*^- \xrightarrow{T_2} e_{aq}^- \qquad (5)$$

Here, e_{free}^- is the precursor of the transient e_*^- species; e_{free}^- was assumed to have no absorptivity at the three wavelengths. The results of the simultaneous parameter estimation at the three wavelengths for this model[23] are shown in Table 1.

Figure 4 shows the reconstruction of the measured kinetic traces of Long *et al.*[9,10] They also found that their measured kinetic traces can be described by the above two-step mechanism. They considered an isosbestic wavelength where the two absorbing electronic species e_*^- and e_{aq}^- would have the same absorptivity, which means that, at that particular wavelength, they are detected as one single absorbing species being formed from the precursor e_{free}^- with a monoexponential law and a characteristic time T_1. They reported finding this monoexponential behavior, *i.e.*, the isobestic wavelength, at 820 nm.[9,10] Table 1 shows the estimated kinetic and optical parameters reported by Long *et al.* to be compared with the results of Gauduel *et al.* We note that these results differ significantly, and the only explanation attributes these differences to the intensity dependence of electron recombination. However, the key point of this argumentation is the independence of the characteristic times T_1 and T_2 from the initial energy of the free electrons, which is not supported by the computer simulations we discuss in this paper (see Table 2 of ref 1).

As we mentioned before, we will compare only these two pump and probe experimental results in detail to simulation results. We will discuss more recent experimental findings only qualitatively in section IV.

III. Comparison of Experiment and Simulation

A. Comparison of the Convolved Kinetic Traces. The most plausible and straightforward method to compare experimentally determined electron hydration kinetics to simulation results would be to compare *deconvolved* (instantaneous) experimental kinetic traces to simulated population curves. To do this, we would need some numerical deconvolution method. However, this direct, "nonparametric" deconvolution of the kinetic functions from the detected convolution is not feasible. All the deconvolution methods that has been studied and published so far work only for data with extremely low experimental noise and a considerably large number (typically more than a thousand) of experimental data points. Now, as we can see from Figure 3, there is a rather large fluctuation in the experimental data, and there are only about 80 points measured at each wavelength. All these features are inherent in the technique of the CPM lasers used; they have a temporal instability and a relatively low pulse repetition rate (usually 10 Hz). As a result, all published deconvolution methods fail to give a reasonable and acceptable kinetic function. From this point of view, the advent of femtosecond solid-state lasers is promising; they work at a few kilohertz repetition rate and also have better temporal stability.

Within the conditions of the available data, the only reliable method that can be used is *reconvolution*.[13] This is practically the inverse of deconvolution; a given kinetic mechanism is supposed prior to the numerical evaluation, and "calculated" (convolved) points are constructed this way. The sum of the squared differences from the measured points can then be minimized to get least-squares estimates for the kinetic parameters contained in the assumed mechanism. Thus, although one cannot get *a priori* instantaneous kinetic functions to compare with simulation results, we can convolve the concentration functions obtained from the simulation to mimic the experimental pump and probe results and compare them to the kinetic traces obtained in the laser experiment.

To do the convolution according to eq 2, we need to know the molar absorptivities (ϵ_i) of all the absorbing species included in mechanism 1. These spectra have been computed with the simulation reported in ref 1. Figure 5 shows the simulated spectra of the species included in mechanism 1. The absorption spectrum of e_{aq}^- is that of the fully relaxed hydrated electron in its s-like ground state. We note that the results manifest a shift of ~0.7 eV to higher energy compared to experiment and a somewhat higher oscillator strength (0.95) than the experimental one.[1] Its maximum value of ~24 000 cm^{-1} M^{-1} is also higher, compared to the experimental 18 500 cm^{-1} M^{-1} value.[14] This shift, characteristic of the simulated solvated electron

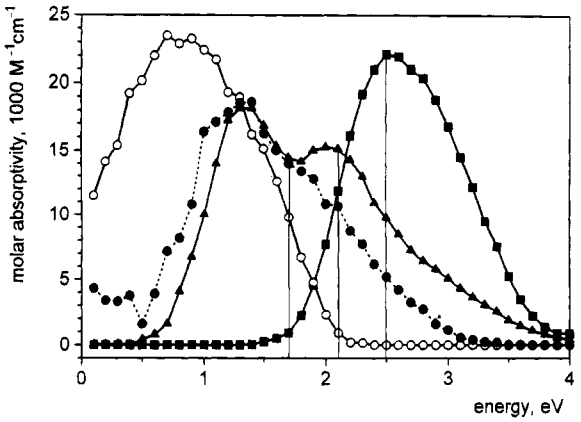

Figure 5. Simulated absorption spectra of the electronic species during electron hydration.[1] ○ denotes the injected excess electron's spectrum with no solvent relaxation. ● is that of the e_{free}^- species in mechanism 1. ▲ and ■ show the spectra of the excited localized e_*^- and the fully relaxed e_{aq}^- species, respectively. Vertical bars indicate the three energies, 1.7, 2.1, and 2.5 eV, used in the comparison to the three experimental wavelengths in Figures 3 and 4.

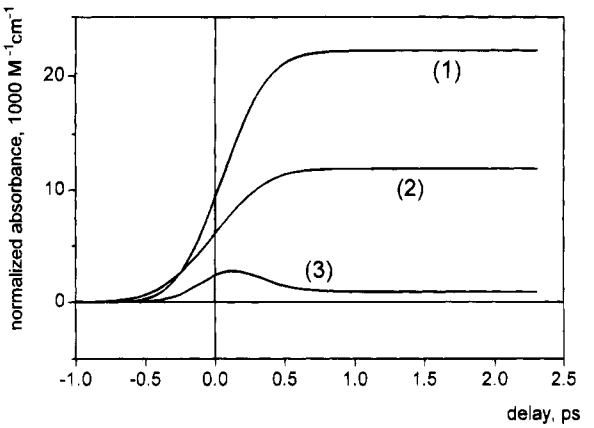

Figure 6. Convolved kinetic traces obtained with the simulated kinetic and absorption parameters[1,2] of the hydration of ~2.5-eV initial excess energy electrons, using the same effective pulses as in Figures 3 and 4. The three curves correspond to those marked with the same number in Figures 3 and 4: (1) at 1.7-eV, (2) at 2.1-eV, and (3) at 2.5-eV photon energies.

spectra and the higher oscillator strength, is very likely contained also in the other three spectra, but they cannot be compared to experimental data. The absorption spectrum denoted by e_{hot}^- is that of the initially created delocalized electron, which has its maximum absorption value around 0.8 eV (≈1600 nm). The spectrum of the species e_{free} was also computed from the configurations of the delocalized electron but after solvent relaxation, the instant before localization. Its maximum is about 1.3 eV (≈1000 nm), and the whole spectrum is largely blue-shifted, compared to the e_{hot}^- spectrum. To calculate the contribution of each absorbing species from e_1^- to e_n^-, the average of the e_{hot}^- and e_{free}^- absorptivities was used. Localization itself brings about not much additional blue shift, as can be seen from the e_*^- spectrum in Figure 5. The latter absorption spectrum shows a reproducible double peak, as noted elsewhere.[1]

All the spectra in Figure 5 are ensemble averages of all the corresponding configurations realized during the simulation, the number of cases ranging from 8 to 20. The points shown are the result of a five-point moving average smoothing procedure. The use of a single spectrum for the absorption of all the species e_1^- to e_n^- is, in fact, in accordance with the computational treatment of mechanism 1, namely, that we suppose a unique charactersistic time T_{th} for each thermalization step, we only get an overall thermalization time for the n "hot" species[2] without distinguishing them.

Another problem encountered in comparing simulation with the experimental pump and probe results is the choice of energy. An equivalent of 720 nm is obviously the maximum energy of the e_{aq}^- spectrum, *i.e.*, about 2.5 eV. The two other energies can be chosen so that they are in reasonable accord with the characteristic relative contributions observed experimentally at longer times. This principle leads to the association of 1.7 and 2.1 eV in the simulation with the experimental wavelengths 1250 and 900 nm, respectively. Alternatively, a simple upward energetic shift by 0.7 eV to obtain suitable simulation energies produces the same result and is also consistent with the assignment of the ground-state absorption maximum. Thus, these choices appear well founded. For the convolution of the simulated results, we used the simulated spectrum of the e_{aq}^- species, while in the evaluation of the experimental curves, we used the experimental e_{aq}^- spectrum.[14]

The results of the simulated convolution are shown in Figure 6. The presence of the transient species is not visually evident in the figure due to their relatively low transient concentrations and to the convolution with the rather broad instrumental response function, with respect to the characteristic times. By comparing the essential features of these convolved kinetic traces (Figure 6) to the experimental ones (Figures 3 and 4), we can conclude that there is less difference between Figure 4 and Figure 6 than between the two experimental results (*i.e.*, Figures 3 and 4). This observation supports the conclusion that the simulation of electron hydration in a water bath of flexible molecules is basically in accordance with the experimental phenomena. The most striking difference is that the simulated traces are developed substantially more rapidly to a steady-state level than the experimental counterparts. Spectral properties—which determine the relative amplitudes of the traces—seem also to be quite different, especially with respect to the experimental traces of Gauduel *et al.* However, it is very important to note that the experimental determination of definite relative intensities at different wavelengths in these ultrafast experiments is extremely difficult, as the irradiation volume unavoidably varies with wavelength. As a result of these difficulties, such absolute intensity data are, in fact, only rarely reported, although it has been provided in the two cases considered here. Therefore, the spectral differences between simulation and experiment (beyond the noted shift) cannot be assigned to limitations of one or the other.

B. Comparison of the Instantaneous Kinetic Curves. The above differences are not as large as could be inferred visually, comparing the convolved kinetic traces. There is another method for the comparison, which is less objective, but is also more informative concerning the details of the mechanism. It is possible to get "instantaneous" population and spectral curves from the experimental data if we suppose a particular mechanism to interpret the results. By use of the method of reconvolution described at the beginning of this section, we can estimate both the kinetic and spectral parameters of this mechanism with a least-squares procedure. As the raw experimental data are available for the kinetic traces of Gauduel *et al.*, we can fit mechanism 1 to these kinetic data to obtain the above parameters. However, there are two reasons why this kind of comparison is less objective than the comparison of the convolved curves. First, here we presuppose mechanism 1 to be valid, which means that any further comparison is only valid within the framework of the mechanism supposed, even if it is not the correct one. Second, as this mechanism is more complicated than the two-step mechanism (eq 5) and, further, the two-step mechanism, which is completely sufficient to fit

the original kinetic traces, is wholly contained in mechanism 1, it is obvious that the fitting of mechanism 1 results in an ill-conditioned parameter estimation. This means that kinetic parameters additional to T_1 and T_2 are not significantly determined by the estimation process. In spite of these difficulties, such an ill-conditioned estimation can be performed and its results can be readily interpreted as the *possibility* that mechanism 1 could be valid within the experimental conditions or, in other words, that experimental results are not inconsistent with the mechanism found in simulation. Now, we can also readily reconstruct concentration functions of mechanism 1 based on the parameters obtained with the above method of estimation. The estimation procedure was based on the Marquardt method, which is described in detail elsewhere.[15] To avoid the above-mentioned ill-conditioned character in the fitting procedure, we included the constraint to keep the absorbance ratio of the different species at the same value as in the simulation, whenever the variation in this ratio did not result in a decrease of the residual error. Even so, the ill-conditioned character precluded obtaining significant values of the parameters, *i.e.*, their uncertainty is usually larger than their actual (mean) value. As a consequence, parameters in the column "Gauduel *et al.*, mechanism 1" of Table 1 should only be taken as a *possible set* of parameters which are, nevertheless, fully in accordance with the experimental data.

To facilitate the comparison, we put together the simulation parameters and the estimated parameters of the thermalization + branching mechanism, as well as the parameters obtained from the experiments with the two-step mechanism in Table 1. (Note that, as original data are not available for the experiments of Long *et al.*, only their published two-step parameters are given.) Figure 7 contains the reconstructed concentration curves of the species e_{hot}^-, e_{free}^-, e_*^-, and e_{aq}^- for the two simulated cases, along with the results from the experimental data sets of Gauduel *et al.* As can be seen from Table 1, the most striking difference here is also that the characteristic times T_2 and T_3 are much shorter in the simulation. Figure 7 reveals more clearly the differences in the time scales; note the 3 times longer scale of the concentration curves of experimental origin. However, there are also striking *similarities* between the simulation of an ~2.5-eV initial energy excess electron hydration and the concentration curves from the experiments of Gauduel *et al.* First of all, it is obvious that the ~2.5-eV initial energy kinetic curves are by far much more similar to the experiment than the ~2-eV initial energy curves. One would say that the only difference—apart from the difference in time scale—is that the channels leading to and from the species e_*^- enable this species to live longer in the experiment than in the simulation. This means a smaller buildup to decomposition ratio $1/92:(1/48 + 1/67) \approx 0.3$ in the simulation, compared to $1/100:(1/330 + 1/350) \approx 1.7$ in the experimental case. (Note that $1/T_i = k_i$ is the rate constant for the monoexponential steps of the formation and the decomposition of e_*^-.) Overall, the comparison of the kinetic curves suggests that the experiment might likely be interpreted with mechanism 1 supposing some 2.5-eV excess energy electrons as precursors and much less likely with the smaller 2-eV excess energy electrons. Furthermore, the *consistency* of mechanism 1 with the experimental results is fully supported by the fit underlying the curves shown in Figure 7.

One is also led to conclude that, since the simulated kinetic curves are sensitive to the initial excess energy of the electrons, differences in the experimental conditions resulting in a comparable difference in the initial energy of the electrons might lead to substantial differences such as those that can be observed between the two sets of experimental results shown in Figures 3 and 4.

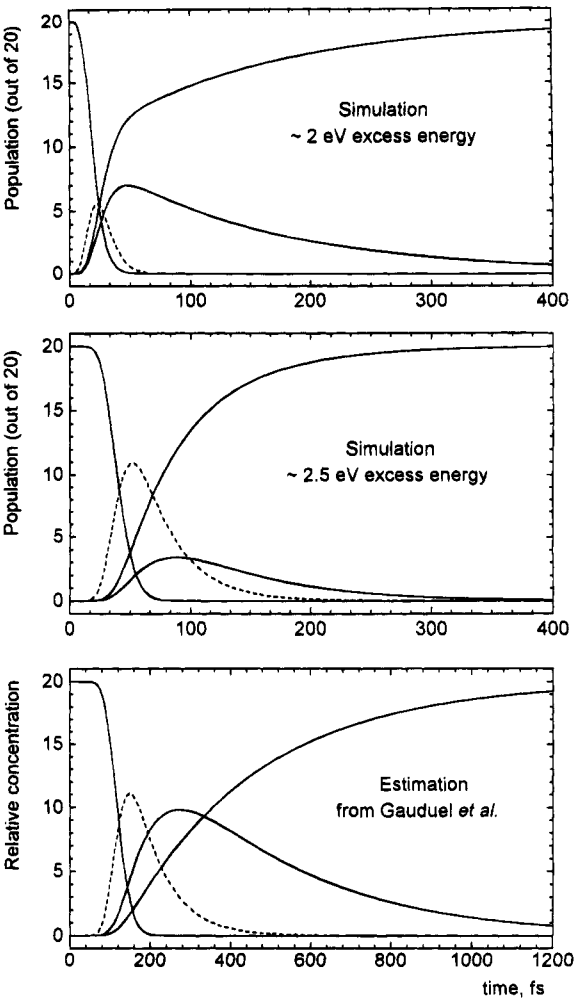

Figure 7. Comparison of the evolution of the (instantaneous) concentration of different electronic species during hydration in the simulation with the two different initial excess energies indicated (upper two diagrams) and in the pump and probe experiment of Gauduel *et al.* (lower diagram), obtained with mechanism 1. The scale for the simulated curves shows the number of electrons out of the total 20 runs, and normalization of the experimental curves to 20 facilitates comparison. Monotonically decreasing curves show the evolution of the sum of all the species from e_1^- to e_n^-, dotted curves show that of the transient e_{free}^-, and the other transient marked with solid curves is e_*^-. The product e_{aq}^- is also marked with solid curves. Note the 3-fold difference of the simulated and the experimental time scales.

IV. Discussion

It is of prime interest to see what we can conclude from the above comparison for the hydration kinetics of electron in pure water within experimental conditions. The most important conclusion is also the most elementary; one should be careful with the interpretation of the experimental kinetic traces in the sense that the most simple mechanism which is sufficient to fully describe the convolved kinetic traces is not necessarily the correct one. The large correlation of the pulse parameters with the spectral and kinetic ones can easily result in a perfect fit of an oversimplified mechanism to the convolved traces. This also means that—unless independent physicochemical evidence would support a particular mechanism—parameters estimated from pump and probe results are to be taken only *within the framework of that particular mechanism*, and not as generally

valid characteristics of the reaction. Now, in the case of electron hydration, physicochemical evidence suggests that we should take into account a nonzero contribution to the absorbance of not only the e_*^- and e_{aq}^- species but also (all the possible) precursor species. The same kind of evidence also suggests that—in contrast to early debates on *whether* the electron localizes in deep, performed traps *or* relaxes after localization[3,17,18]—we should consider *both* hydration channels. As the simulations discussed here are based on first principles computations, we should take their results to positively support the hypothesis that both the precursors' spectral contribution and the branching between the two hydration channels are significant. In fact, later experimental results obtained with higher precision measurements revealed that the two-step mechanism is insufficient to fully account for the observed kinetic traces.

On the basis of the interpretation of their results on electron hydration in concentrated aqueous solutions,[6] Gauduel *et al.* also supposed an alternative to the two-step mechanism. In concentrated (11 M) HCl solutions, they found a broad peak in the transient spectra at some 930 nm which, after 2 ps, has about the same amplitude as the usual e_{aq}^- peak at 720 nm.[6] They attribute it to the spectrum of an "encounter pair" $(H_3O^+ \cdots e^-)_{hyd}$. By analogy, they include the above encounter pair in the hydration mechanism in pure water as another (parallel) two-step hydration channel, primarily to account for the absorption at longer wavelengths. This second channel assumes a branching including an independent fast recombination.[7] The overall mechanism can be written in the form

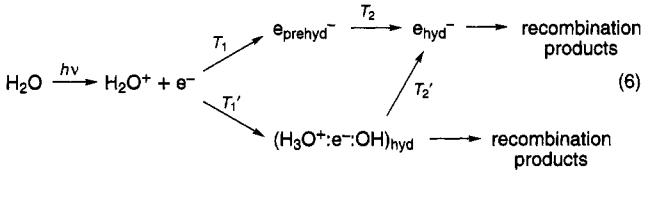

(6)

The idea of an encounter pair dates back to the early papers on diffusion-controlled reactions.[19,20] The concept was used to refer to a critical distance of encounter R, within which reaction occurred between the two encountering species, *i.e.*, it was an *operational* unit rather than a structural unit. Czapski and Peled[21] proposed that, if we suppose the encounter pair to be a "reactive configuration" of the two species and we attribute a finite lifetime plus the possibility of separation without reaction to this configuration, this would readily explain "slower than diffusion-controlled" electron scavenging reaction rates in concentrated solutions of some scavengers (as $H_3O_{aq}^+$). However, Lam and Hunt[22] wrote in a subsequent paper that "The ps pulse radiolysis studies in other solvents (than water) have indicated that the encounter pair model does not seem to explain the fast electron process". The issue is still open as to whether an encounter pair has the structural properties to produce a distinct signature via its optical absorption spectrum. (Keszei and Jay-Gerin made a somewhat similar suggestion[23] considering an *ion pair* $H_2O^+ \cdots e^-$ in the photoionization process of water, but an ion pair *is* a structural entity rather than operational entity.)

The idea of "another hydration channel" was also supposed by Lewis and Jonah, in a paper on scavenging reactions of solvated electrons in 1-propanol and ethanol.[24] They could qualitatively explain their results supposing the existence of two precursors of the solvated electron, according to the mechanism

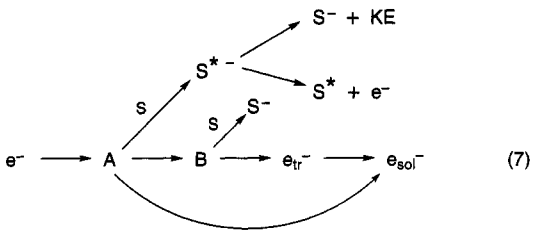

(7)

The unspecified states A and B should not be thought of as well-defined states but as encompassing a distribution of energies (A has higher energy than B).

A third idea to explain electron hydration dynamics has been proposed by Barbara *et al.*, namely, local temperature rise due to the action of ionizing laser pulses.[25] Though it was in the context of a multiple pulse experiment to excite freshly formed hydrated electrons, such a mechanism could account for a continuous shift of the absorption of electronic species due to the local temperature change during electron hydration itself.

Several authors also suggested the idea of a continuous blue shift of the spectrum of a localized electron during the hydration process. Messmer and Simon[26] interpreted the results of Gauduel *et al.*,[4] which we have used in section III, based on a mixture of a two-step hydration and a continuous blue shift mechanism. Recent experiments on anion[27] and electron[28] solvation in alcohols have also been interpreted on the basis of a continuous blue shift due the (long range) rearrangement of the solvent molecules around the freshly localized electron.

Here, we would like to point out that there is much in common among the four mechanisms cited and mechanism 1 proposed here. These common features are that *more than two* absorbing *species* are supposed to contribute to the measured absorption and *more than one solvation channel* is supposed to exist. Little rearrangement is needed to show the equivalence of the interpreting power of those mechanisms. If we drop the terminating recombination steps of scheme 6, we have a very similar process to mechanism 1:

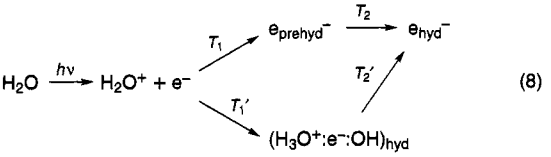

(8)

If we increase the number of absorbing species *before branching* and assume that the absorbing species $(H_3O^+:e^-:OH)_{hyd}$ does not produce a distinct spectral contribution, we obtain

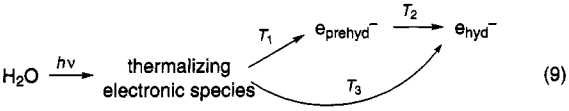

(9)

which is just the same as mechanism 1. From the point of view of the explanative power, mechanisms 6 and 9 are roughly equivalent. There is even less rearrangement needed to make the solvation part of scheme 7

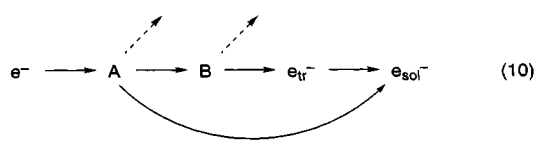

(10)

completely equivalent to mechanism 1. All that is needed is to displace the branching point from A to B and then to include several species between A and B as a compensation to keep its rationalizing power—and we have again mechanism 1. The "continuous blue shift" interpretations, in fact, fully coincide with the n-step thermalization prior to branching, in accordance

with the gradually blue-shifted spectra of the thermalizing electronic species prior to localization, found in simulation.[1]

Obviously, there are marked differences from a physicochemical point of view between the mechanisms discussed, even if they are rather similar from a computational or interpretative point of view. As a recent interesting example of computationally equivalent mechanisms, we could cite the interpretation of electron-scavenging reactions in methanol *on the basis of ion pairing*[29] and its reinterpretation *without the hypothesis of ion pairing* on the basis of the role of the changing ion atmosphere.[30] Independent experiments on the existence of ion pairs obviously could decide this issue. Correspondingly, future experiments need to be carried out for the present case. However, for the time being, mechanism 1, proposed on the basis of simulation, is the only mechanism based on more than rationalization; it is supported by the first principles method of simulation, whose results are independent of experimental ones.

It is of great future interest to pursue a detailed analysis of the cited, or more recent results, in cooperation with the authors of the experimental results on electron solvation in water and alcohols to evaluate the validity of the mechanism, obtained in the simulation, within experimental conditions.

Acknowledgment. E. Keszei gratefully acknowledges the support of a grant by the National Research Fund of Hungary under Contract OTKA 4187, as well as computational support of the IBM Academic Initiative in Hungary. P. J. Rossky acknowledges the support of the National Science Foundation and the Robert A. Welch Foundation.

References and Notes

(1) Murphrey, T. H.; Rossky, P. J. *J. Chem. Phys.* **1993**, *99*, 515.
(2) Keszei, E.; Nagy, S.; Murphrey, T. H.; Rossky, P. J. *J. Chem. Phys.* **1993**, *99*, 2004.
(3) Wiesenfeld, J. M.; Ippen, E. P. *Chem. Phys. Lett.* **1980**, *73*, 47.
(4) Migus, A.; Gauduel, Y.; Martin, J. L.; Antonetti, A. *Phys. Rev. Lett.* **1987**, *58*, 1559.
(5) Gauduel, Y.; Pommeret, S.; Migus, A.; Antonetti, A. *Radiat. Phys. Chem.* **1989**, *34*, 5; *J. Phys. Chem.* **1989**, *93*, 5.
(6) Gauduel, Y.; Pommeret, S.; Migus, A.; Antonetti, A. *J. Am. Chem. Soc.* **1990**, *112*, 2925.
(7) Pommeret, S.; Antonetti, A.; Gauduel, Y. *J. Am. Chem. Soc.* **1991**, *113*, 9105. Gauduel, Y.; Pommeret, S.; Antonetti, A. *J. Phys. Chem.* **1993**, *97*, 134.
(8) Long, F. H.; Lu, H.; Eisenthal, K. B. *J. Chem. Phys.* **1989**, *91*, 4413.
(9) Long, F. H.; Lu, H.; Eisenthal, K. B. *Phys. Rev. Lett.* **1990**, *64*, 1469.
(10) Long, F. H.; Lu, H.; Eisenthal, K. B. *J. Opt. Soc. Am.* **1990**, *B7*, 1511.
(11) Pépin, C.; Houde, D.; Remita, H.; Goulet, T.; Jay-Gerin, J.-P. *Phys. Rev. Lett.* **1992**, *69*, 3389.
(12) Keszei, E.; Jay-Gerin, J.-P. *Radiat. Phys. Chem.* **1989**, *33*, 183.
(13) McKinnon, A. E.; A. Szabó, G.; Miller, D. R. *J. Phys. Chem.* **1977**, *81*, 1564.
(14) Hart, E. J.; Anbar, M. *The Hydrated Electron*; Wiley: New York, 1970.
(15) Press, W. H.; Flannery, B. P.; Teukolsky, S. A.; Vetterling, W. T. *Numerical Recipes, The Art of Scientific Computing*; Cambridge University: Cambridge, MA, 1986.
(16) Long, F. H.; Lu, H.; Shi, X.; Eisenthal, K. B. *Chem. Phys. Lett.* **1991**, *185*, 47.
(17) Gauduel, Y.; Martin, J. L.; Migus, A. G.; Yamada, N.; Antonetti, A. In *Ultrafast Phenomena V*; Fleming, G. R., Siegman, A. E. Eds.; Springer: Berlin, 1986; pp 308–311.
(18) Kenney-Wallace, G. A.; Jonah, C. D. *J. Chem. Phys.* **1982**, *86*, 2572.
(19) Smoluchowski, M. V. *Z. Phys. Chem.* **1917**, *92*, 129.
(20) Debye, P. *Trans. Electrochem. Soc.* **1942**, *82*, 265.
(21) Czapski, G.; Peled, E. J. *Phys. Chem.* **1973**, *77*, 893.
(22) Lam, K. Y.; Hunt, J. W. *Int. J. Radiat. Phys. Chem.* **1975**, *7*, 333.
(23) Keszei, E.; Jay-Gerin, J. P. *Can. J. Chem.* **1992**, *70*, 21.
(24) Lewis, M. A.; Jonah, C. D. *J. Phys. Chem.* **1986**, *90*, 5367.
(25) Kimura, Y.; Alfano, J. C.; Walhout, P. K.; Barbara, P. F. *J. Phys. Chem.* **1994**, *98*, 3450.
(26) Messmer, M. C.; Simon, J. D. *J. Phys. Chem.* **1990**, *94*, 1220.
(27) Lin, Y.; Jonah, C. D. *J. Phys. Chem.* **1993**, *97*, 295.
(28) Pépin, C.; Houde, D.; Goulet, T.; Jay-Gerin, J.-P. *J. Phys. Chem.* **1994**, *98*, 7009.
(29) Duplâtre, G.; Jonah, C. D. *J. Phys. Chem.* **1991**, *95*, 897.
(30) Kang, T. B.; Freeman, G. R. *Can. J. Chem.* **1993**, *71*, 1297.

JP940424D